

Supporting information

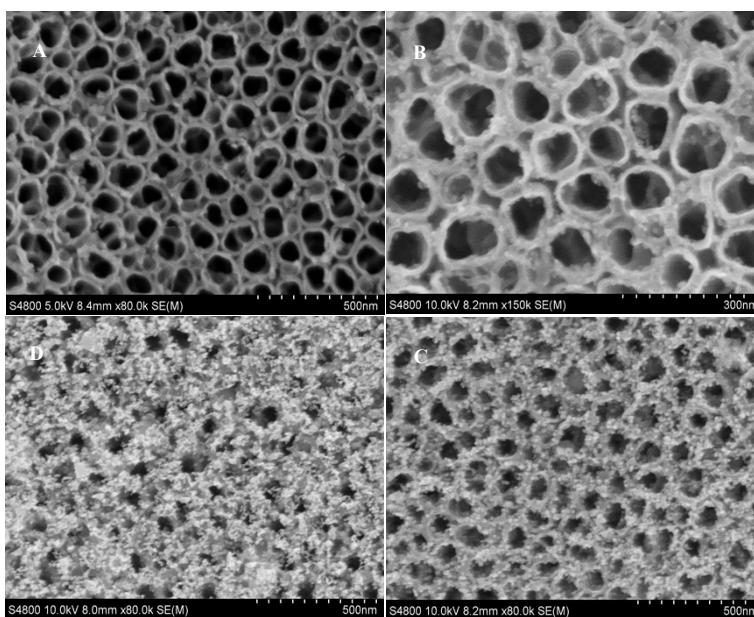


Figure S1 (A)-(D): SEM images of CuInSe₂ modified-TiO₂ NTAs with one, two, four and five dipping-coating cycles

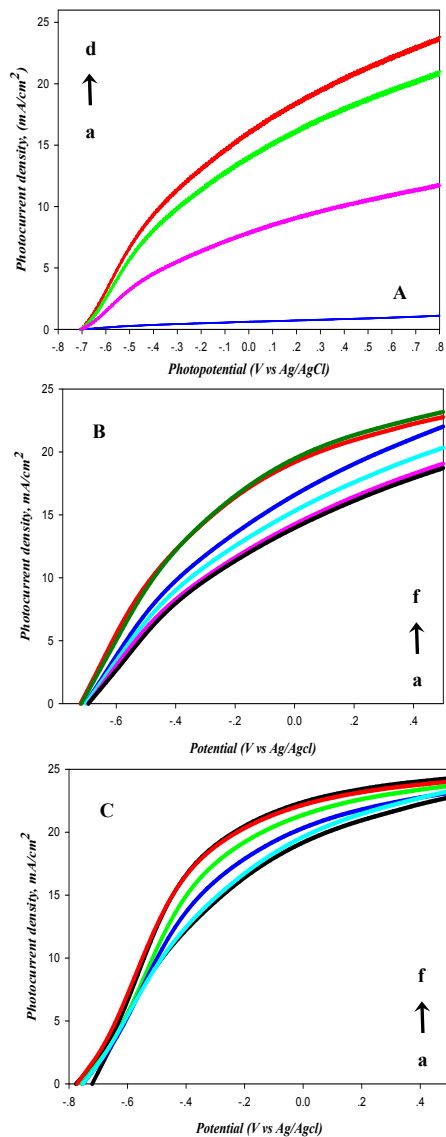


Figure S2 A: CuInSe₂ nanocrystals- sensitized TiO₂ NTAs photoelectrode with one to three dipping-coating cycles (a to d) under one sun illumination. B: optimization of CdS-Mn coating layer, from curve a to f: 0, 1, 4, 7, 10 and 13. C: optimization of double ZnS coating layers, from curve a to f: 0, 1, 3, 5, 7 and 9.

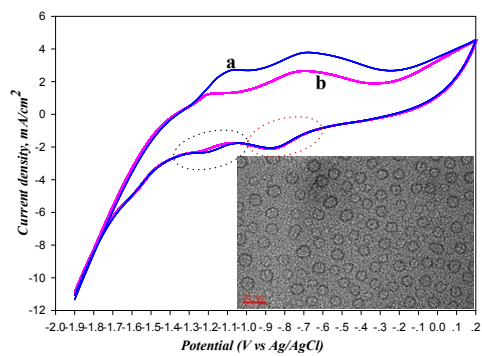


Figure S3 Cyclic voltammogram records of TiO_2 NTAs/ CuInSe_2 /CdS-Mn photoelectrode with 10 layers Mn-CdS layers. Particularly, for curves a and b were recorded with 25 and 12 nm hollow CuInSe_2 nanocrystals, respectively. Inset shows the TEM image of 25 nm hollow CuInSe_2 nanocrystals.

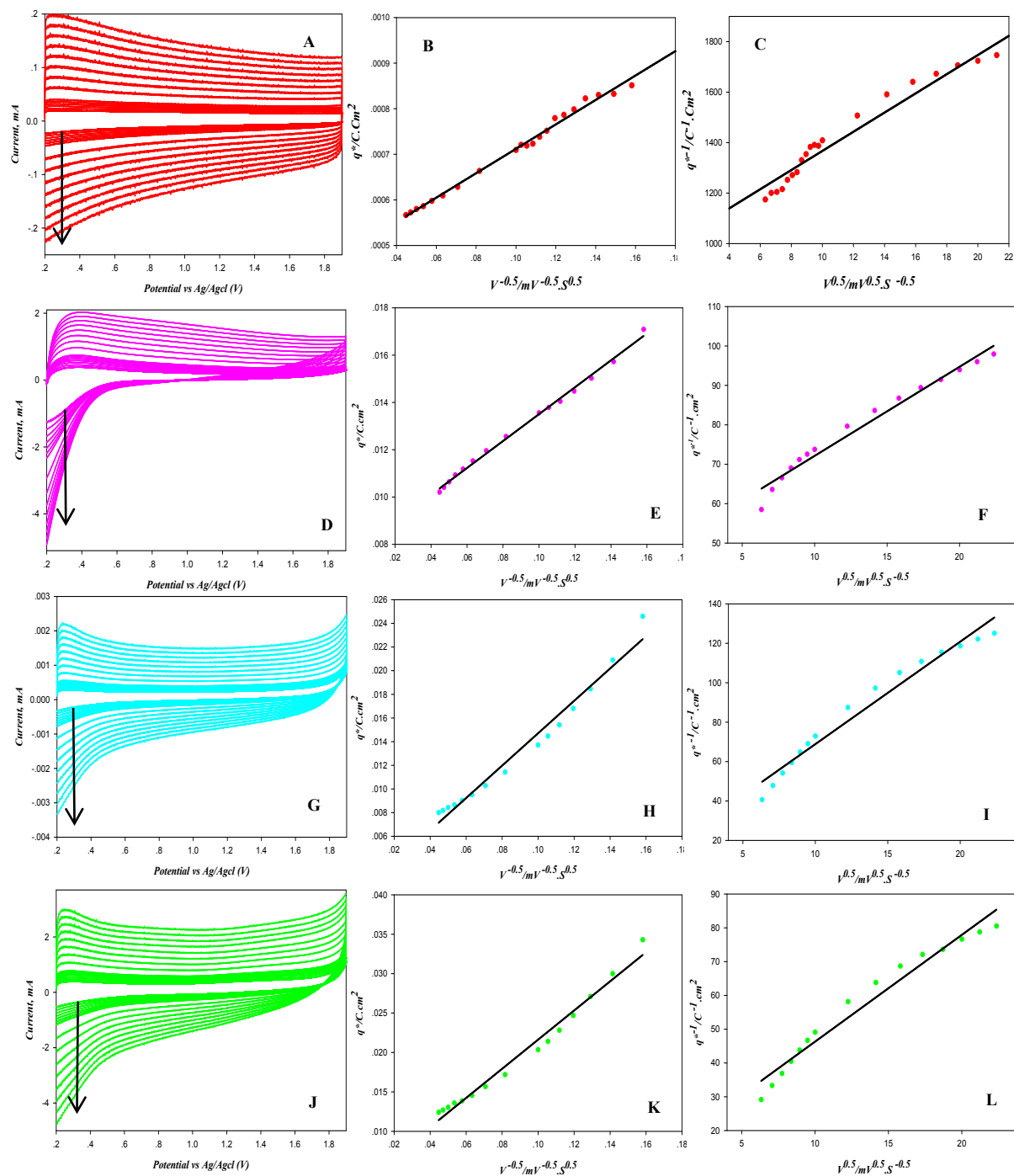


Figure S4. Cyclic voltammograms, plots q^* at scan rate V as a function of $V^{-0.5}$ and l/q^* at scan rate V as a function of $V^{0.5}$ of different photoelectrodes: A, B, C: naked TiO_2 NTAs; D, E and F: TiO_2 NTAs/ CuInSe_2 ; G, H and I: TiO_2 NTAs/ CuInSe_2 / CdS-Mn ; J, K and L: TiO_2 NTAs/ ZnS/CuInSe_2 - CdS-Mn/ZnS . All cyclic voltammetry measurement are recorded in 0.5 M H_2SO_4 in the potential region from 0.2 to 0.9 V with scan rates from 40, 50, 60, 70, 80, 90, 100, 150, 200, 250, 300, 350, 400, 450 to 500 mV^{-1} . Arrow indicate the increase of scan rates.

Quantum well structure exists in the inner of the TiO₂ NTAs:

Because, it is very difficult to directly characterize the internal multilayer structure through the wall of the TiO₂ NTAs. Here, we develop a structure model (Scheme 1) to analyze the element distribution dependence on the location, then, to indirectly confirm internal multilayer structure, as follow:

For horizontal nanotube (Scheme 1), there are two walls at middle region under a top-down view, the upper and down walls. There are two surfaces for each wall: inner and outer surfaces. However, there is only one wall, including two outer surfaces (upper outer surface and down outer surface) in the marginal region. And both the inner and outer surfaces can equally load sensitizers. So, once the electron beam focus on the middle region for STEM assay, there will be four layers sensitizers, display a higher brightness with elements mapping assay compared with marginal region (two layers sensitizers).

With the help of this model, one can successfully confirm the structure ZnS/TiO₂ NT (Fig 4C and D): middle region own higher brightness for both Ti and O elements due to double walls (the upper and down walls). After introduction of ZnS (pre-treatment), the elements distribution for both Zn and S still agree well with this model (regions III and IV of Fig 4E; Fig 4F). So, we firmly believe that ZnS exist inner the TiO₂ NT, in addition to the outer wall. Based on this fact, one can believe that double layers ZnS can be directly decorated onto the inner and outer surfaces of TiO₂ NTAs with SILAR and this decoration method is also suitable to the following introduction of CdS and ZnS (pre-treatment) layers.

In Fig 5C, the brightness of element Cu (from CuInSe₂) in middle region (region IV) is higher than marginal region (region V), indicates that the inner surface of TiO₂ NT are well covered by hollow CuInSe₂ nanocrystals, which agree well the top morphology of the CuInSe₂/ZnS/TiO₂ NTAs in Fig 3B. Similar brightness difference of different elements (Figures G, H and I) in middle region and marginal region also indicates the inner decoration. More important, as shown in Fig 3C and Fig 3D (red arrows), hollow CuInSe₂ nanocrystals no longer disperse directly on the ZnS/TiO₂ NTAs (same as in Fig 3B), but are covered with a film. This fact further confirm that this quantum well structure exist in the inner of the TiO₂ NTAs.